Structural phase transition in single-crystal $CH_3NH_3CdBr_3$: I. Experimental studies

1992 J. Phys.: Condens. Matter 4 7179

(http://iopscience.iop.org/0953-8984/4/35/004)

J. Phys.: Condens. Matter 4 (1992) 7179–7190. Printed in the UK

Structural phase transition in single-crystal $CH_3NH_3CdBr_3$: I. Experimental studies

A Kallel†, Y Mlik†, C Courseille‡ and M Couzi§

† Departement de Physique, Ecole Nationale des Ingénieurs de Sfax, Route de Soukra, 3038 Sfax, Tunisia

‡ Laboratoire de Cristallographie et de Physique Cristalline, Université de Bordeaux I, 33405 Talence Cédex, France

§ Laboratoire de Spectroscopie Moléculaire et Cristalline, Université de Bordeaux I, 33405 Talence Cédex, France

Received 6 February 1992

Abstract. Single crystals of $CH_3NH_3CdBr_3$ (MACB) have been studied as a function of temperature by means of differential scanning calorimetry, x-ray diffraction and Raman scattering measurements. A first-order structural phase transition is evidenced by all three techniques at 170 K. The high-temperature phase (I) is hexagonal, with space group $P6_3/mmc$ and $Z = 2$ formula units per unit cell. The x-ray diffraction patterns of the low-temperature phase (II) are consistent with a complex orthorhombic unit cell with lattice parameters such as $a_{II} \simeq 4a_{hex}$, $b_{II} \simeq 2\sqrt{3}a_{hex}$ and $c_{II} \simeq 3c_{hex}$, i.e. corresponding to $Z = 96$; however, it is shown that the system can be described in a simplified manner by means of an orthorhombic 'projection' unit cell onto the hexagonal plane with parameters such as $a_p \simeq a_{hex}$, $b_p \simeq \sqrt{3}a_{hex}$ and $c_p \simeq 3c_{hex}$. The Raman data clearly indicate that the phase transition is of the order–disorder type, owing to the reorientational processes of the methylammonium groups.

1. Introduction

The crystal of formula $CH_3NH_3CdBr_3$ (MACB) belongs to a group of compounds exhibiting a marked one-dimensional type of structure, of which $(CH_3)_4NMnCl_3$ (TMMC) has been probably the most widely studied from the points of view of its magnetic and structural properties [1–4 and references cited therein].

The phase of MACB stable at room temperature is hexagonal, with space group $P6_3/mmc$ and $Z = 2$ formula units per primitive unit cell; the lattice parameters are $a = b = 7.897$ Å and $c = 6.888$ Å [5]. This corresponds to the prototype phase for all compounds of this series [1–3]. The structure consists of infinite chains made of face-sharing $CdBr_6$ octahedra, running parallel to the c (hexad) direction. The space between chains is occupied by the methylammonium (MA) groups, which are situated on sites with D_{3h} symmetry at (1/3, 2/3, 3/4) and (2/3, 1/3, 1/4) [5]. This site symmetry is incompatible with the C_{3v} symmetry of the free MA groups, so that these latter necessarily exhibit orientational disorder, so as to achieve statistically the D_{3h} symmetry. In fact, examination of Fourier difference maps [5] reveals that the C–N bonds are tilted with respect to the c direction, probably because of the influence of NH···Br hydrogen bonds between the polar NH_3 ends of the MA groups and the bromine atoms of the octahedral chains. As a result, the instantaneous

0953-8984/92/357179+12$04.50

position of the MA group conserves one σ_v mirror plane as a unique symmetry element, which means that the D_{3h} site symmetry is achieved by the superposition of six energetically equivalent orientations, as represented schematically in figure 1; three of these orientations have the NH_3 end oriented 'up', and the other three orientations correspond to NH_3 oriented 'down'. Thus, the reorientational dynamics of the MA groups in the hexagonal phase of MACB can be described in the frame of a multidimensional pseudo-spin model [6] of complex nature, i.e. including six positions for the MA groups on each site.

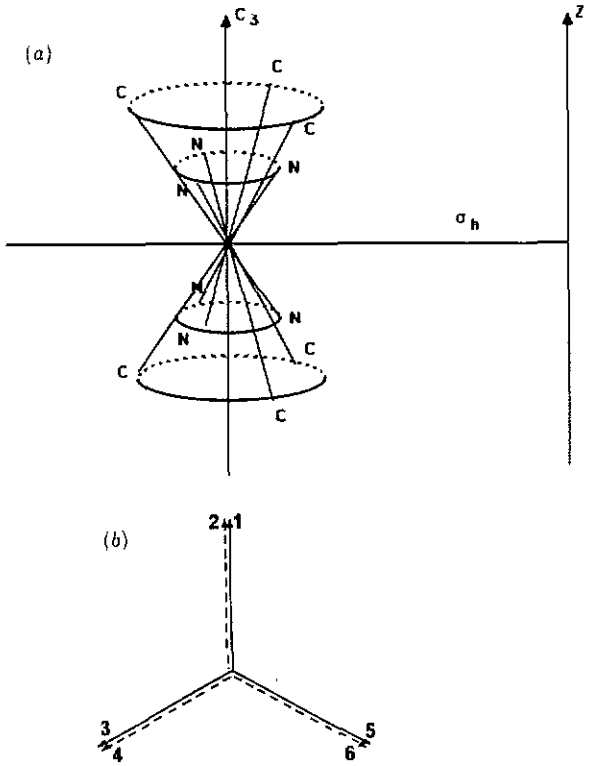

Figure 1. Schematic representation of the six orientations of the $CH_3NH_3^+$ groups of MACB in the hexagonal phase, generating statistically a site with D_{3h} symmetry (from [5]). (*a*) Projection along direction perpendicular to *c*. (*b*) Projection along the *c* direction. Full lines, MA group oriented 'up' (1, 3, 5). Broken lines, MA group oriented 'down' (2, 4, 6).

A phase transition occurring around 170 K has been reported in MACB [1]; however, to our knowledge, this phase transition has not been analysed so far, in the absence of data concerning the structure of the low-temperature phase.

The aim of the present work is to gain information on the nature of this phase transition. Our results will be presented in a series of two papers, hereafter referred to as I and II, respectively. This paper (I) is devoted to an experimental study of MACB as a function of temperature, by means of differential scanning calorimetry (DSC), single-crystal x-ray diffraction and Raman scattering experiments. In paper II [7], a transition mechanism will be tentatively given, on the basis of a pseudo-spin formalism developed in the frame of group theory.

2. Experimental details

2.1. Sample preparation

Single crystals of MACB have been prepared by slow evaporation at room temperature of a saturated aqueous solution containing stoichiometric amounts of CH_3NH_3Br and $CdBr_2 \cdot 4H_2O$; the solution was slightly acidified by adding a few drops of HBr. Colourless single crystals in the shape of a prism elongated along the hexagonal axis are obtained, with dimensions up to 2 mm × 2 mm × 3 mm; they have been used for Raman scattering experiments. Much smaller crystals have been selected for x-ray diffraction measurements.

2.2. Differential scanning calorimetry measurements

Differential scanning calorimetric measurements have been performed on a Dupont DSC model 910/990. The rates of increasing and decreasing temperature were 1 or 2 K min^{-1}, and the temperature range explored extends from 77 to 300 K; the powdered samples, about 2 mg, were put into hermetically sealed metal capsules.

2.3. X-ray diffraction

Powder x-ray diffraction experiments as a function of temperature (80–300 K) have been performed with a Guinier Simon camera from Enraf Nonius, using the Cu K_α radiation obtained with a quartz monochromator.

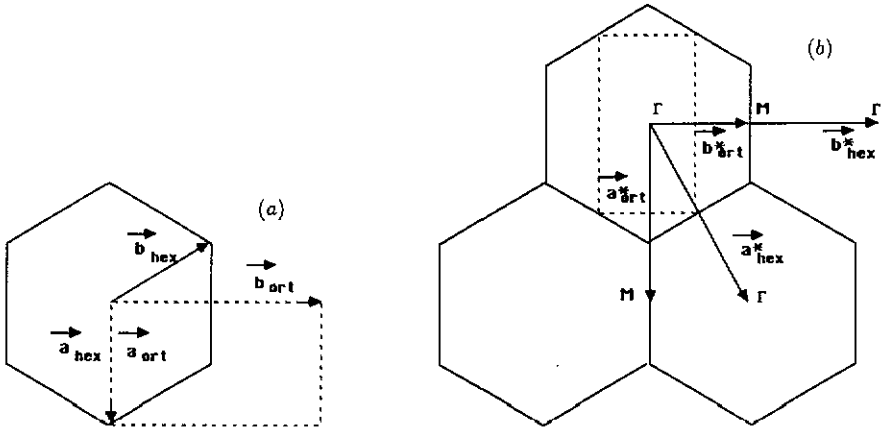

Figure 2. The relations between the hexagonal (hex) and orthorhombic (ort) axes: (*a*) in direct space; (*b*) in reciprocal space.

Single crystals of MACB have been studied with Weissenberg and precession cameras, using the Mo K_α radiation obtained with a graphite monochromator. Low-temperature measurements, down to 120 K, were achieved by means of an Enraf Nonius nitrogen gas flow system. As will be shown in section 3.2 the low-temperature phase of MACB exhibits an orthorhombic symmetry; the relations between hexagonal and orthorhombic axes are given in figure 2. Hence, if $h\,k\,l$ designate the Miller indices related to a^*_{hex}, b^*_{hex} and c^*_{hex} and $h'k'l'$ those related to a^*_{ort} b^*_{ort} and c^*_{ort} (c^*_{hex}), there exist the following relations: $h' = h$, $k' = h + 2k$, $l = l'$.

For precession photographs at low temperature, three different scattering configurations have been adopted. In the first one, the x-ray beam was set parallel to c^*_{ort} (c^*_{hex}) so as to observe diffraction planes parallel to (a^*_{ort}, b^*_{ort}), corresponding also to (a^*_{hex}, b^*_{hex}) planes. In the second one, the a^*_{ort} axis was set parallel to the incident x-ray beam, allowing the observation of planes parallel to (b^*_{ort}, c^*_{ort}), corresponding also to (b^*_{hex}, c^*_{hex}) planes (figure 2). Finally, the crystal was rotated by 90° around c_{ort} (c_{hex}), so that the incident x-ray beam was parallel to b^*_{ort}, allowing the observation of planes parallel to (a^*_{ort}, c^*_{ort}) or equivalently (a^*_{ort}, c^*_{hex}).

2.4. Raman scattering

The Raman spectra have been recorded with either a Dilor Z24 or a Coderg T800 triple monochromator instrument, coupled with a Spectra Physics argon-ion laser model 171. The 514.5 nm emmision line was used for excitation with incident power not exceeding 0.2 W in order to avoid crystal damage. A Dilor C4N nitrogen continuous flow cryostat was used to keep the sample at different temperatures stabilized between 80 and 300 K. Spectra were also recorded down to 20 K with a Cryodine model 20 helium refrigerator, equipped with the sample holder modification described in [8]. In both cases, the temperature regulation was better than ±0.5 K.

The X, Y, Z orthogonal laboratory axes chosen for single-crystal measurements correspond to the a_{ort} (a_{hex}), b_{ort} and c_{ort} (c_{hex}) directions, respectively, as defined in figure 2.

3. Results and discussion

3.1. Differential scanning calorimetry measurements

Numerous cycles of heating and cooling between 77 and 300 K always reveal a strong thermal anomaly at about 170 K, related to the phase transition previously reported [1]. In the limit of experimental accuracy, no thermal hysteresis could be detected; however the DSC signal exhibits the characteristic shape of a first-order transformation. This first-order character will be further confirmed by means of x-ray diffraction and Raman scattering experiments.

3.2. X-ray diffraction

Guinier Simon photographs of MACB exhibit marked discontinuities in the thermal evolution of a number of diffraction lines around 170 K, consistent with the occurrence of a first-order structural phase transition. However, from these data, it is still very hard to gain precise information on the symmetry of the low-temperature phase.

Weissenberg and precession photographs of single-crystal MACB taken at room temperature confirm the hexagonal symmetry and the $P6_3/mmc$ space group [5], owing to the systematic absence of $0\,0\,l$ ($l = 2n + 1$) and $h\,h\,l$ ($l = 2n + 1$) reflections [9]. The unit-cell parameters at room temperature determined from both single-crystal and powder data are $a_{hex} = b_{hex} = 7.902$ Å and $c_{hex} = 6.888$ Å, in good agreement with Fuess's data [5].

Single-crystal data obtained through Weissenberg and precession photographs in the low-temperature phase (phase II) at about 120 K reveal a huge number of superstructure reflections, which were absent in the hexagonal phase (phase I) at room temperature.

First, a trebling of the lattice parameter along the c_{hex} direction is clearly evidenced on Bragg photographs taken with the crystal rotating around the hexagonal axis. It is worth noting that a similar phenomenon has already been reported in the low-temperature phases of the related compounds $(CH_3)_4NCdCl_3$ (TMCC) [2] and $(CH_3)_4NCdBr_3$ (TMCB) [10].

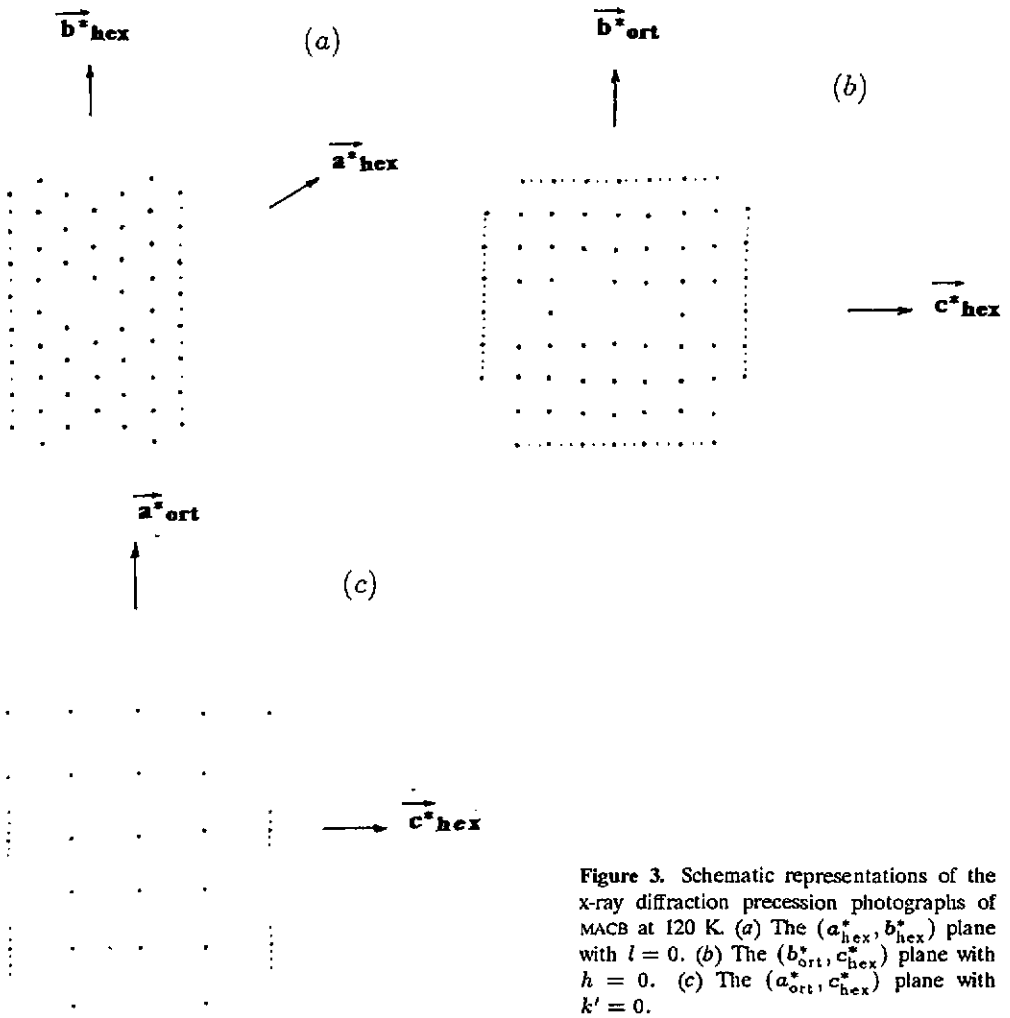

Figure 3. Schematic representations of the x-ray diffraction precession photographs of MACB at 120 K. (*a*) The (a^*_{hex}, b^*_{hex}) plane with $l = 0$. (*b*) The (b^*_{ort}, c^*_{hex}) plane with $h = 0$. (*c*) The (a^*_{ort}, c^*_{hex}) plane with $k' = 0$.

Figure 3(*a*) shows the diffraction patterns of the (a^*_{hex}, b^*_{hex}) plane with $l = 0$ obtained at 120 K with the precession camera. The main Bragg peaks of the hexagonal phase I are still observed, as expected, and new superstructure reflections along the b^*_{ort} (b^*_{hex}) direction are evidenced, situated at the M point (0, 1/2, 0) of the hexagonal Brillouin zone [11]. This means already that phase II is also characterized by a doubling of the unit cell occurring in the hexagonal plane, leading to an orthorhombic unit cell with parameters corresponding to a_{ort}, b_{ort} (figure 2), thus replacing the M point at zone centre [12]. It is important to notice that the superstructure reflections

are observed along one direction only, whereas there are three equivalent $\Gamma - M$ directions in the hexagonal system [11], which would lead to the existence of three equivalent orthorhombic domains (ferroelastic domains) oriented at 120° from each other. Apparently, our data show that one of these domains is strongly predominant in phase II of MACB, possibly due to an uncontrolled internal and/or external strain applying to the crystal.

The precession photographs of the (b^*_{ort}, c^*_{hex}) plane with $h = 0$ is shown in figure 3(*b*). The trebling of the c parameter is confirmed by the observation of superstructure reflections on row lines parallel to c^*. In addition superstructure reflections are also observed on row lines parallel to b^*_{ort} (b^*_{hex}), in particular on the $l = 4$ row line, which are consistent with a doubling of the b_{ort} lattice parameter such as defined in figure 2. Note that these superstructure reflections include the M point of the Brillouin zone, as reported already in figure 3(*a*).

In figure 3(*c*) is shown the precession photograph of the (a^*_{ort}, c^*_{hex}) plane with $k' = 0$. Again superstructure reflections are observed along the a^*_{ort} direction, in particular on the $l = 4$ row line; this leads to the existence of a quadrupling of the a_{ort} lattice parameter.

Altogether, these results lead to a 'giant' orthorhombic unit cell for phase II, with lattice parameters such as $a_{II} \simeq 4a_{hex}$, $b_{II} \simeq 2b_{ort} = 2\sqrt{3}a_{hex}$ and $c_{II} \simeq 3c_{hex}$, i.e. a unit cell corresponding to $Z = 96$ formula units. Clearly, owing to the complexity of this unit cell, it would be interesting to find a simplified description of the system. Indeed, as already mentioned, the (a^*_{hex}, b^*_{hex}) plane, with $l = 0$ (figure 3(*a*)) only reveals a doubling of the unit cell in the hexagonal plane. Now it is important to point out that this $l = 0$ plane is the Fourier transform of the structure in direct space projected onto the hexagonal plane [13]. In other words, the complex orthorhombic unit cell of phase II, when projected along the c direction, only reveals a doubling of the hexagonal unit cell in the hexagonal plane, such as represented in figure 2. Thus, in the following and in particular in paper II, we shall define a 'projection' unit cell with parameters such as $a_p \simeq a_{ort} = a_{hex}$, $b_p \simeq b_{ort} = \sqrt{3}a_{hex}$ and $c_p \simeq 3c_{hex}$. Hence, we conclude that the quadrupling of a_{ort} on the one hand, and the doubling of b_{ort} on the other hand, as observed in the actual structure of phase II, are necessarily due to complex atomic displacements along the c axis, which cannot influence the 'projection' structure in the hexagonal plane. Note also that the present data do not reasonably allow us to propose a space group for the complex orthorhombic structure of phase II, nor for the 'projection' structure.

3.3. Raman scattering

The Raman spectra of MACB single crystals have been studied in the low-frequency range (0–200 cm^{-1}) corresponding to the 'lattice vibrations'; spectra have also been recorded in the frequency range around 900–1000 cm^{-1} corresponding to the C–N stretching vibration of the MA groups. The so-called lattice vibrations correspond to all vibrational modes of the $CdBr_6$ octahedral chains and to the external modes of the MA groups, i.e. to their rotatory and translatory vibrations. From classical factor-group analysis [14], the representation of the lattice vibrations at the Brillouin zone centre of MACB in the hexagonal phase I is the following:

$$\Gamma = A_{1g} + 2A_{2g} + 2B_{1g} + 2E_{1g} + 3E_{2g} + 3A_{2u} + 2B_{1u} + 2B_{2u} + 4E_{1u} + 3E_{2u}.$$

This enumeration includes the $k = 0$ acoustic modes (of zero frequency), which transform as $A_{2u} + E_{1u}$. Among the even-parity (g) modes, only the A_{1g} ($\alpha_{xx} +$

α_{yy}, α_{zz}), E_{1g} (α_{xz}, α_{yz}) and E_{2g} ($\alpha_{xx} - \alpha_{yy}$, α_{xy}) ones are expected to be Raman-active [15]. These latter can be described as follows [1–3]:

(i) The totally symmetric A_{1g} mode corresponds to a breathing vibration of the octahedral chains (stretching-like).

(ii) The two E_{1g} vibrations are respectively an internal bending mode of the octahedra and a degenerate rotatory mode of the MA groups around axes perpendicular to *c*.

(iii) The E_{2g} representation contains two internal (bending-like) modes of the octahedral chains and a translatory vibration of the MA groups along directions perpendicular to the hexagonal axis.

At this stage, it is important to notice that the selection rules reported above refer to the averaged structure of MACB in phase I, i.e. with the MA groups having the D_{3h} site symmetry. Now, as stressed in section 1, this site symmetry results from orientational disorder of the MA groups; under these conditions, in addition to the allowed $k = 0$ modes, the Raman spectra may exhibit disorder-induced scattering [16, 17], i.e. may reflect a weighted frequency distribution of phonon modes throughout the whole Brillouin zone ($k \neq 0$).

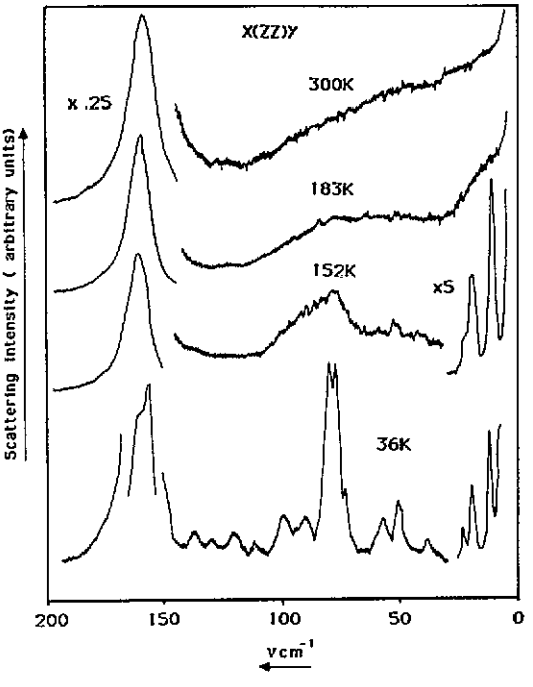

Figure 4. The low-frequency α_{zz} Raman spectrum of MACB as a function of temperature.

The low-frequency Raman spectra of MACB single crystals as a function of temperature are shown in figures 4 to 6. From a general point of view, the spectra recorded in the hexagonal phase, i.e. above $T_c = 170$ K, exhibit broad features as expected for a disordered phase. Abrupt changes occur at the transition temperature, which are consistent with a first-order transition, and then the spectra progressively reveal numerous narrow lines as the temperature decreases from 170 down to 20 K.

3.3.1. Hexagonal phase I. In phase I, the A_{1g} (α_{zz}) spectrum is dominated by a strong

line at 160 cm^{-1} (figure 4), assigned to the expected breathing mode of the octahedral chains. This frequency compares nicely with the corresponding one observed at 156 cm^{-1} in TMCB [1, 18]. In addition, we observe a broad band extending from 0 to 100 cm^{-1}, which corresponds to disorder-induced scattering, i.e. to a frequency distribution of low-lying phonon modes. A similar feature has already been reported in the high-temperature hexagonal phase ($P6_3/mmc$) of TMMC and TMCC [2]. In the case of MACB, this frequency distribution splits into two parts, which are more clearly perceptible at low temperature just above T_c (figure 4); the first one, appearing at $\simeq$ 20 cm^{-1} as a shoulder on the Rayleigh line, may be due to acoustic-like chain modes at $k \neq 0$, and the second one, centred around 70 cm^{-1}, is more likely due to external vibrations of the disordered MA groups.

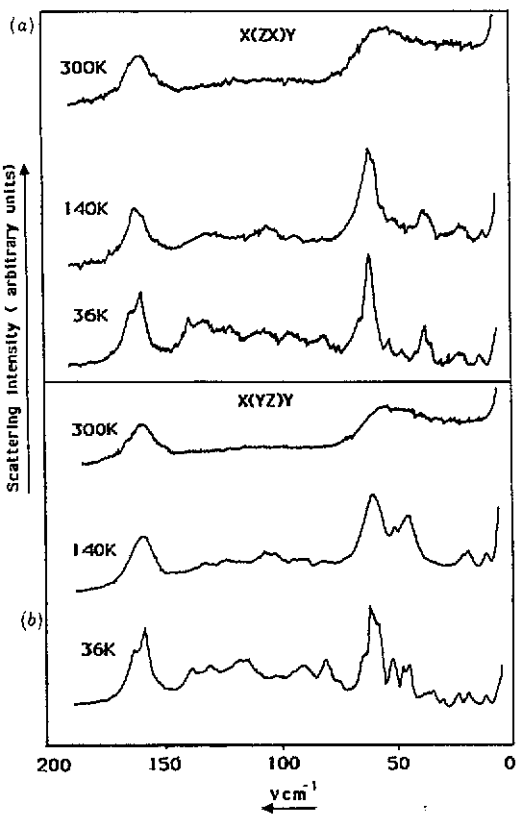

Figure 5. The low-frequency α_{xz} (*a*) and α_{yz} (*b*) Raman spectra of MACB as a function of temperature.

The E_{1g} (α_{xz}, α_{yz}) spectra (figures 5(*a*) and (*b*)) exhibit a plateau-like scattering at low frequency, ending in a broad band at 50 cm^{-1}. Certainly, 'disorder-induced' scattering strongly contributes to these spectra, even though two E_{1g} modes at $k = 0$ are expected according to the averaged symmetry. Note the presence of a weak line at 160 cm^{-1} due to a polarization leakage of the strong A_{1g} line occurring at this frequency.

The three expected modes with E_{2g} symmetry are observed on the α_{xy} spectrum (figure 6) at about 50, 110 and 130 cm^{-1}, respectively; again they appear as broad and partially resolved features (note also a weak polarization leakage of the strong

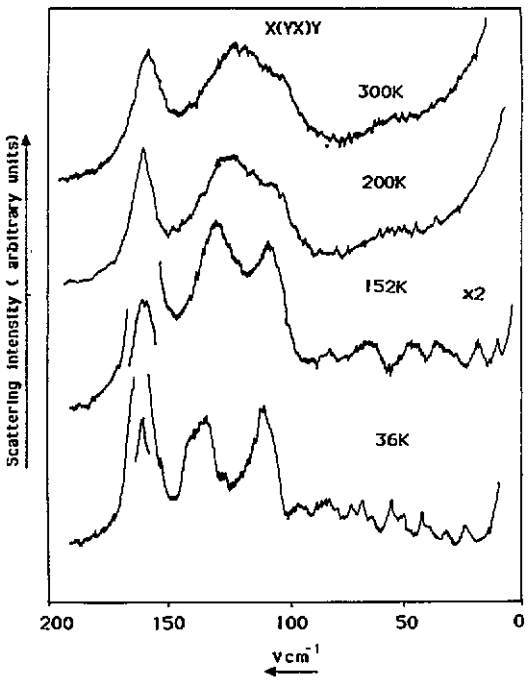

Figure 6. The low-frequency α_{xy} Raman spectrum of MACB as a function of temperature.

A_{1g} mode at 160 cm^{-1}). The E_{2g} spectrum is further characterized by the presence of a strong quasi-elastic scattering ('Rayleigh wing') that we assign to jump motions of the MA groups between different orientations. Indeed, as will be shown in paper II [7], among the pseudo-spin coordinates attached to the reorientations of the MA groups, two of them transform according to the E_{2g} degenerate representation at zone centre. It is worth noting that this representation corresponds to the e_1-e_2 and e_6 components of the strain tensor in the $6/mmm$ (D_{6h}) crystalline class [19]; e_1-e_2 is the only component able to induce a low-temperature (ferroelastic) phase II with orthorhombic symmetry [12, 19]. A similar situation was encountered with crystals of TMMC and TMCC [2–4], but in those cases quasi-elastic scattering was completely absent in the E_{2g} Raman spectrum; this was attributed to the T_d (spherical) symmetry of the $(CH_3)_4N^+$ groups in TMMC and TMCC, whose reorientations cannot produce any change of the crystal polarizability [3]. Thus, it is heartening to point out that in the case of the MA groups with C_{3v} point symmetry (rod-like shape), reorientations of the CN bonds may indeed produce a variation of polarizability resulting in quasi-elastic scattering as observed in the disordered phase of MACB.

3.3.2. Orthorhombic phase II. Because of the complex orthorhombic unit cell found for phase II of MACB, and in the absence of space-group determination, the Raman spectra can be discussed on qualitative grounds only. Anyhow, whatever the space group of phase II could be, the number of observed Raman lines at low temperature is far less than can be expected for such a unit cell with $Z = 96$, or even for the simplified 'projection' unit cell with $Z = 12$.

One of the most striking changes occurring abruptly at $T_c \simeq 170$ K is observed on the α_{zz} spectrum (figure 4), where the weak broad band of phase I at $\simeq 20$ cm^{-1} gives rise in phase II to a set of three very strong and narrow lines at 11, 19 and

21 cm^{-1}, respectively. These low-lying modes are probably due to transverse and/or longitudinal acoustic modes (involving mainly motions of $CdBr_6$ octahedral chains) at those points of the Brillouin zone ($k \neq 0$ in phase I) which are replaced at zone centre in phase II. The point Δ (0, 0, 1/3), associated with the trebling of the lattice parameter along c, and the point M (0, 1/2, 0) that defines the 'projection' unit cell, are good candidates. Furthermore, the frequency distribution at $\simeq 70$ cm^{-1} is progressively replaced by a number of narrow lines; note also the splitting of the breathing mode of the octahedral chains (160 cm^{-1}) at low temperature (figure 4).

The plateau-like scattering of the α_{xz} and α_{yz} spectra abruptly disappears in phase II where it is replaced by weak but well defined features (figure 5). It is important to notice that the α_{xz} (figure 5(*a*)) and α_{yz} (figure 5(*b*)) spectra are markedly different in phase II. This is indeed expected for a biaxial crystal (orthorhombic in our case), provided that the sample remains essentially single-domain. This result corroborates our observations by x-ray diffraction.

The quasi-elastic scattering of the α_{xy} spectrum completely disappears below T_c (figure 6), and again this spectrum progressively gives rises to a great number of Raman lines as the temperature is lowered.

To summarize, all these results are consistent with the occurrence of a first-order transition at 170 K; it is certainly of the order–disorder type since the broad frequency distributions and quasi-elastic scattering characteristic of the disordered phase I are replaced by well defined features in phase II. However, in spite of the first-order character of the transition, a number of Raman lines remain rather broad just below T_c (figures 4 to 6), which means that some kind of residual disorder still persists before the system becomes completely ordered as the temperature is lowered down to $\simeq 20$ K.

3.3.3. The stretching mode of the MA group. The α_{zz} Raman spectra of phases I and II of MACB recorded in the 900–1000 cm^{-1} frequency range (i.e. corresponding to the CN internal stretching mode of the MA groups) are shown in figure 7. In phase I a single line at $\simeq 970$ cm^{-1} is observed, whereas in phase II at least three components at 967, 971 and 973 cm^{-1}, respectively, can be resolved. These three components must be assigned to crystal-field splitting and/or to the existence of three sets of inequivalent MA groups in phase II. Again, this result is consistent with an ordered structure for phase II.

4. Conclusions

The experimental studies of crystals of $CH_3NH_3CdBr_3$ by means of differential scanning calorimetry and x-ray diffraction and Raman scattering measurements as a function of temperature show that a first-order phase transition occurs at $T_c \simeq 170$ K. The hexagonal symmetry of the high-temperature phase I is confirmed and the x-ray diffraction patterns obtained in the low-temperature phase II reveal a huge number of superstructure reflections, which are consistent with a giant orthorhombic unit cell. It is shown, however, that this complex system can be described in a simplified manner by means of a 'projection' unit cell onto the hexagonal plane; this unit cell is still orthorhombic. The Raman data show that the mechanism of the transition at T_c is essentially of the order–disorder type, due to ordering processes of the methylammonium groups; indeed, the MA groups are orientationally disordered between six

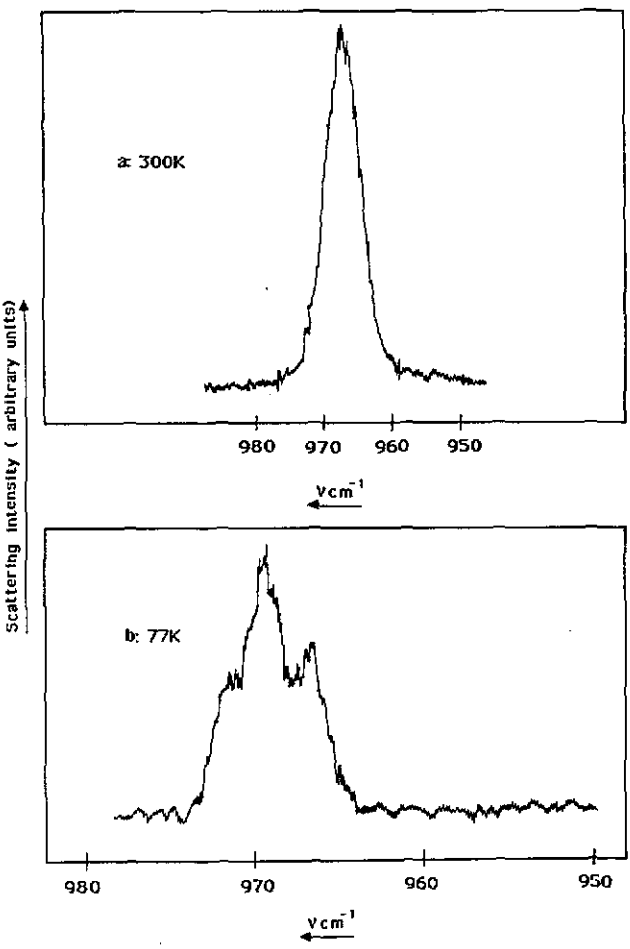

Figure 7. The CN stretching mode of the methylammonium groups of MACB: (*a*) phase I (300 K); (*b*) phase II (77 K).

equivalent positions in phase I, leading to the observation of broad frequency distributions and quasi-elastic scattering, and these features are replaced by well defined Raman lines in the ordered phase II. The ordering processes of the MA groups will be tentatively analysed in paper II.

Acknowledgments

The authors wish to thank Professor H Fuess (Technishe Hochschule, Darmstadt, Germany) for communication of the structure determination of phase I prior to publication. We are also indebted to Drs N B Chanh and C Hauw (UA 144, CNRS, University of Bordeaux I) for valuable experimental help and useful discussions. MC would like to thank the 'Region Aquitaine' for providing us with a part of the Raman equipment used in this study. This work has been supported by a French–Tunisian cooperation programme under the form of grants attributed to AK.

References

[1] Mlik Y 1981 *Thesis* University of Tunis
[2] Braud M N, Couzi M, Chanh N B, Courseille C, Gallois B, Hauw C and Meresse A 1990 *J. Phys.: Condens. Matter* **2** 8209
[3] Braud M N, Couzi M, Chanh N B and Gomez Cuevas A 1990 *J. Phys.: Condens. Matter* **2** 8229
[4] Braud M N, Couzi M and Chanh N B 1990 *J. Phys.: Condens. Matter* **2** 8243
[5] Fuess H, private communication, to be published
[6] Couzi M, Negrier Ph, Poulet H and Pick R M 1988 *Croat. Chem. Acta* **61** 649
[7] Kallel A, Mlik Y and Couzi M 1992 *J. Phys.: Condens. Matter* **4** 0000
[8] Cavagnat R, Cornut J C, Couzi M, Daleau G and Huong P V 1978 *Appl. Spectrosc.* **32** 500
[9] *International Tables for Crystallography* vol A *Space Group Symmetry* 1984 ed T Hahn (Dordrecht: Reidel)
[10] Aguirre Zammalloa G, Couzi M, Chanh N B and Gallois B 1990 *J. Physique* **51** 2135
[11] Bradley C J and Cracknell A P 1972 *The Mathematical Theory of Symmetry in Solids* (Oxford: Clarendon)
[12] Stokes H T and Hatch D M 1988 *Isotropy Subgroups of the 230 Crystallographic Space Groups* (Singapore: World Scientific)
[13] Cowley J M 1975 *Diffraction Physics* (Amsterdam: North-Holland) pp 112–4
[14] Turrell G C 1972 *Infrared and Raman Spectra of Crystals* (London: Academic)
[15] Poulet H and Mathieu J P 1970 *Spectres de Vibration et Symetrie des Cristaux* (Paris: Gordon and Breach)
[16] Pick R M 1972 *Proc. Congr. Physics of Impurity Centres in Crystals (Tallinn)* p 293
[17] Couzi M, Sokoloff J B and Perry C H 1973 *J. Chem. Phys.* **58** 2965
[18] Aguirre Zamalloa G and Couzi M 1992 in preparation
[19] Salje E K H 1990 *Phase Transitions in Ferroelastic and Coelastic Crystals* (Cambridge: Cambridge University Press)